ChemPubSoc Europe

DOI: 10.1002/chem.201805616

CHEMISTRY A European Journal Full Paper

Organic Electronics

Molecular Design Approach Managing Molecular Orbital Superposition for High Efficiency without Color Shift in Thermally Activated Delayed Fluorescent Organic Light-Emitting Diodes

Mounggon Kim[+],[a] Seong-Jun Yoon[+],[a] Si Hyun Han[+],[b] Ramin Ansari,[c] John Kieffer,[a] Jun Yeob Lee,*[b] and Jinsang Kim*[a]

Abstract: Molecular design principles of thermally activated delayed fluorescent (TADF) emitters having a high quantum efficiency and a color tuning capability was investigated by synthesizing three TADF emitters with donors at different positions of a benzonitrile acceptor. The position rendering a large overlap between the highest occupied molecular orbital (HOMO) and the lowest unoccupied molecular orbital (LUMO) enhances the quantum efficiency of the TADF emitter. Regarding the orbital overlap, donor attachments at 2- and 6-positions of the benzonitrile were more beneficial than 3- and 5-substitutions. Moreover, an additional attachment of a weak donor at the 4-position further increased the quantum efficiency without decreasing the emission energy. Therefore, the molecular design strategy of substituting strong donors at the positions allowing a large molecular orbital overlap and an extra weak donor is a good approach to achieve both high quantum efficiency and a slightly increased emission energy.

Introduction

There has been a great improvement in the external quantum efficiency (EQE) of organic light-emitting diodes (OLEDs) over the last 20 years, which was mostly driven by phosphorescent OLED technology enabling 100% triplet exciton harvesting efficiency.[1–7] However, the use of precious Ir in the molecular structure is not cost-effective, which inspired the development of purely organic-based thermally activated delayed fluorescence (TADF)[8–16] and metal-free organic phosphors[17–20] as an alternative to the organometallic phosphors.

Numerous TADF materials have been devised based on basic design rules to manipulate the singlet transition process and triplet exciton up-conversion process. The molecular design approach for the efficient singlet transition process and triplet up-conversion process is self-contradictory because the first process requires a large HOMO–LUMO overlap, whereas the second process demands a large HOMO–LUMO separation. However, the conflicting requirements can be resolved by rational design of TADF chemical structure. The most common design is based on a donor–acceptor chemical platform, particularly, a multiple donor type structure,[8,12,21–24] a dual emitting core structure,[25–27] and a multiple resonance type donor–acceptor structure.[28] These chemical approaches are proven to be effective by demonstrating a high EQE of over 20% and a high photoluminescence (PL) quantum yield close to 100%. Especially, the multiple donor type designs, such as (4s,6s)-2,4,5,6-tetra(9*H*-carbazol-9-yl) isophthalonitrile (4CzIPN)[8,29–32] and 9,9′,9′′-(5-(4,6-diphenyl-1,3,5-triazin-2-yl)benzene-1,2,3-triyl)tris(9*H*-carbazole) (TCzTrz),[33] are most popular as the main building block of the TADF emitters. Inclusion of multiple donors in the TADF molecules is known to increase the HOMO–LUMO overlap and to reduce the singlet-triplet energy gap (ΔE_{ST}). Consequently, a high singlet transition efficiency and a reverse intersystem crossing (RISC) efficiency are simultaneously achievable in those molecules. However, one unanswered question is the effect of the donor position in the molecular structure on the light-emitting performance, although the multiple donors themselves enhance the light emission efficiency. The substitution position effects of the donor have been reported for host materials[34,35] and TADF emitters containing a single donor.[36,37] However, reports discussing the donor position effect in TADF emitters with multiple donors are very rare, and there has been no systematic investigation. Moreover, the inclusion of an additional donor unit tends to redshift the wavelength of the resulting TADF molecule, which makes it challenging to develop high efficiency TADF emitters

[a] *Dr. M. Kim,[+] S.-J. Yoon,[+] Prof. J. Kieffer, Prof. J. Kim*
Department of Materials Science and Engineering
University of Michigan, Ann Arbor, Michigan 48109 (USA)
E-mail: jinsang@umich.edu

[b] *S. H. Han,[+] Prof. J. Y. Lee*
School of Chemical Engineering, Sungkyunkwan University
2066, Seobu-ro, Jangan-gu
Suwon, Gyeonggi, 440-746 (Korea)
E-mail: leej17@skku.edu

[c] *R. Ansari*
Department of Chemical Engineering
University of Michigan, Ann Arbor, Michigan 48109 (USA)

[+] *These authors contributed equally to this work.*

Supporting information and the ORCID identification number(s) for the author(s) of this article can be found under: https://doi.org/10.1002/chem.201805616.

with a short emission wavelength. Therefore, it is meaningful to explore the molecular design approach for enhancing the efficiency while keeping the same emission spectrum.

Herein, we designed and synthesized TADF emitters composed of multiple phenoxazine donors and a benzonitrile acceptor. Very recently, Adachi and co-workers reported deep-blue TADF emitters containing multiple carbazole donors and a benzonitrile acceptor, in which the donor strength of the substituted carbazole was shown to play an important role in the TADF properties but the connection position of carbazole donors was not investigated.[38] In this work, the connection position of the phenoxazine donors to the benzonitrile acceptor was managed and the effect of the donor position on the TADF characteristics was examined. Comparison of the three TADF emitters, 2,6-di(10*H*-phenoxazin-10-yl)benzonitrile (*o*-CNPhe), 3,5-di(10*H*-phenoxazin-10-yl)benzonitrile (*m*-CNPhe), and 4-(diphenylamino)-2,6-di(10*H*-phenoxazin-10-yl)benzonitrile (*o*-CNPheAm), indicated that 2- and 6-substitution of donors is more effective than 3- and 5-substitution in enhancing EQE of the TADF devices. Moreover, additional attachment of a relatively weak diphenylamine donor at the 4-position of the benzonitrile further increased the EQE of the devices without lowering the emission energy. The demonstrated substitution-position-dependent EQE of the TADF devices is well correlated with the molecular orbital superposition of the TADF emitters.

Results and Discussion

The three TADF molecules, *o*-CNPhe, *m*-CNPhe, and *o*-CNPheAm, have a benzonitrile acceptor and phenoxazine donors or a mixed donor of phenoxazine and diphenylamine. The *o*-CNPhe and *m*-CNPhe are similar in that they have two phenoxazine donors attached to the benzonitrile, but at different substitution positions (2 and 6 in *o*-CNPhe, 3 and 5 in *m*-CNPhe). The *o*-CNPheAm has an additional diphenylamine donor at the 4-position of the *o*-CNPhe. The three emitters are designed to study the effect of the substitution position linked to the molecular orbital superposition on the TADF emission characteristics.

Synthetic pathways to *o*-CNPhe, *m*-CNPhe, and *o*-CNPheAm are shown in Scheme 1. The three molecules were simply prepared by one- or two-step reaction procedures. Final yields of *o*-CNPhe, *m*-CNPhe, and *o*-CNPheAm were 82, 72, and 54%, respectively. All molecules were purified using a vacuum train sublimation procedure to over 99% purity (see Figure S1 in the Supporting Information for the purity confirmation).

The HOMO and LUMO distribution were calculated using the basic set of B3LYP/6-311+G** in the Gaussian 09 program and the molecular orbital calculation outputs of *o*-CNPhe, *m*-CNPhe, and *o*-CNPheAm are shown in Figure 1 together with the results of calculations on the benzonitrile acceptor (see Table S1 in the Supporting Information for the summary of TD-DFT calculations). Given that the benzonitrile is an acceptor of the TADF emitters, the LUMO distribution is important for the TADF emission characteristics. The LUMO calculations show that the LUMO is localized on the 1- and 4-positions of the

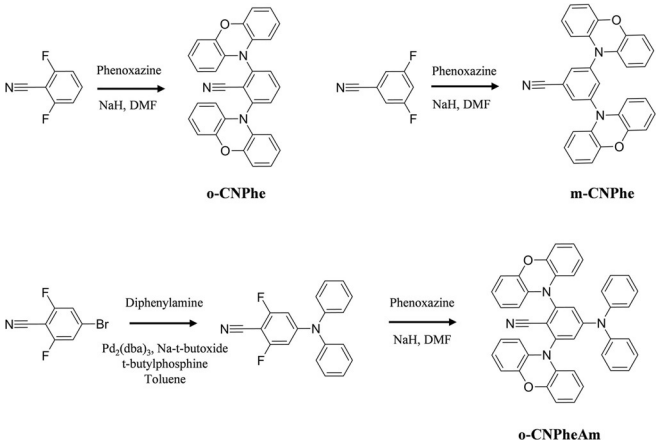

Scheme 1. Synthetic Scheme of *o*-CNPhe, *m*-CNPhe, and *o*-CNPheAm.

phenyl ring, and the 2- and 6-positions have higher LUMO density than the 3- and 5-positions. Comparing the 1- and 4-positions, the 1-position has a rather large contribution to the LUMO density. In the design of the TADF emitters, the HOMO and LUMO overlap is critical to the radiative transition process from the singlet excited state to the ground state. The HOMO and LUMO overlap is extensive when the donors placed at the substitution positions have strong LUMO character. Therefore, the molecular orbital picture of benzonitrile suggests that the substitution of donors at the 2-, 6-, and 4-positions of benzonitrile would increase the radiative transition probability.

The HOMO and LUMO pictures of *o*-CNPhe and *m*-CNPhe indicate that the HOMO–LUMO superposition mostly occurs on the benzonitrile acceptor. The HOMO–LUMO overlap of *o*-CNPhe is possible at the 2-, and 6-positions of benzonitrile, whereas that of *m*-CNPhe is enabled at the 3- and 5-positions of benzonitrile. It can be presumed from the molecular orbital data that the *o*-CNPhe would have better HOMO–LUMO overlap for efficient singlet emission than *m*-CNPhe. In the case of *o*-CNPheAm, the HOMO and LUMO distribution of the frontier orbital of *o*-CNPheAm was similar to that of *o*-CNPhe, but there is additional contribution to the HOMO–LUMO overlap by the triphenylamine unit at the 4-position. Therefore, the *o*-CNPheAm is anticipated to perform better than the other two emitters in the singlet emission process.

Photophysical characterization of the TADF emitters is important to correlate the structure of TADF emitters with light absorption and emission properties. UV/Vis and photoluminescence (PL) characterization of *o*-CNPhe, *m*-CNPhe, and *o*-CNPheAm are compared in Figure 2(a). UV/Vis absorption spectra of the *o*-CNPheAm reflected its extended conjugation by showing redshifted absorption peak and a strong charge transfer (CT) character by exhibiting absorption over 350 nm owing to the additional diphenyl amine at the 4-position. The maximum absorption coefficients (ε) of the three molecules were $0.94\times10^5\,M^{-1}cm^{-1}$ for *o*-CNPhe, $0.87\times10^5\,M^{-1}cm^{-1}$ for *m*-CNPhe, and $0.92\times10^5\,M^{-1}cm^{-1}$ for *o*-CNPheAm.

Room temperature PL (fluorescence) and low temperature PL (phosphorescence)[38,39] of the three TADF emitters were measured to characterize the emission properties and the sin-

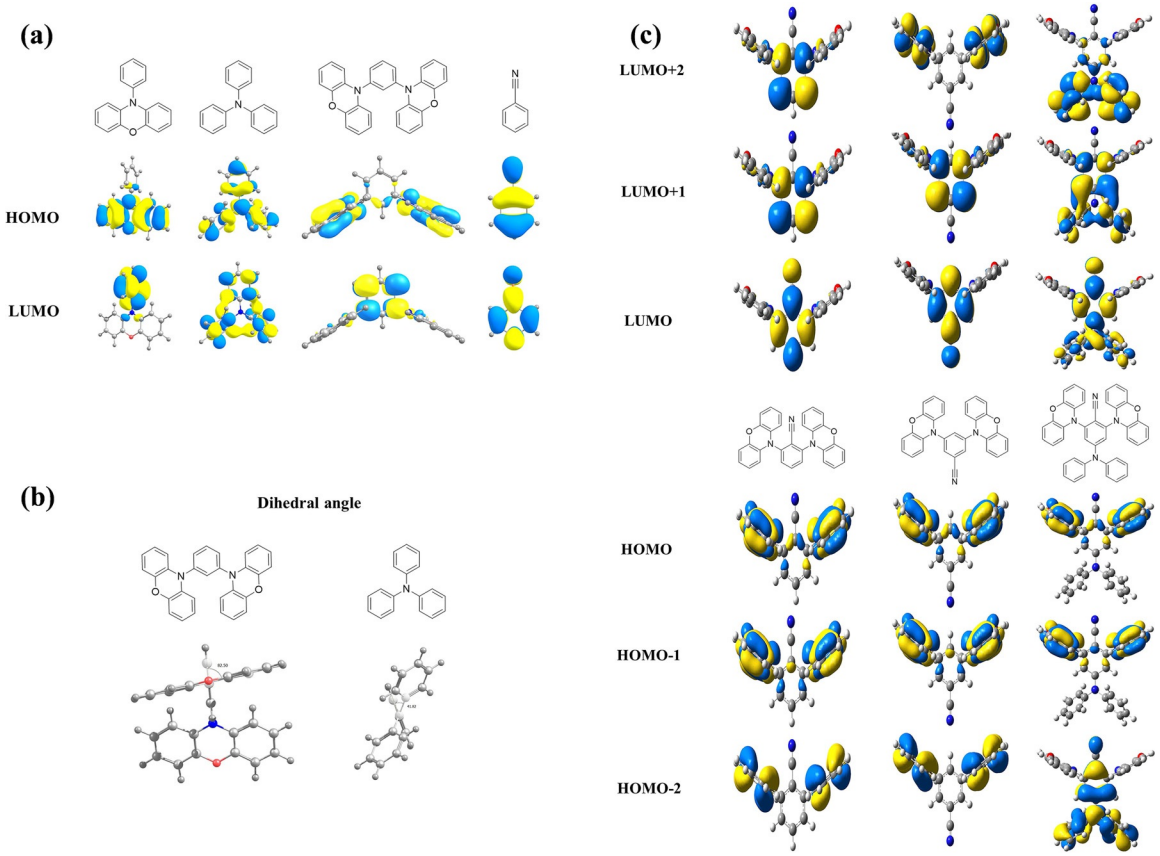

Figure 1. a) The HOMO and LUMO distribution of the donor and acceptor molecules. b) The dihedral angle of donor molecules. c) The HOMO and LUMO distribution of *o*-CNPhe, *m*-CNPhe, and *o*-CNPheAm.

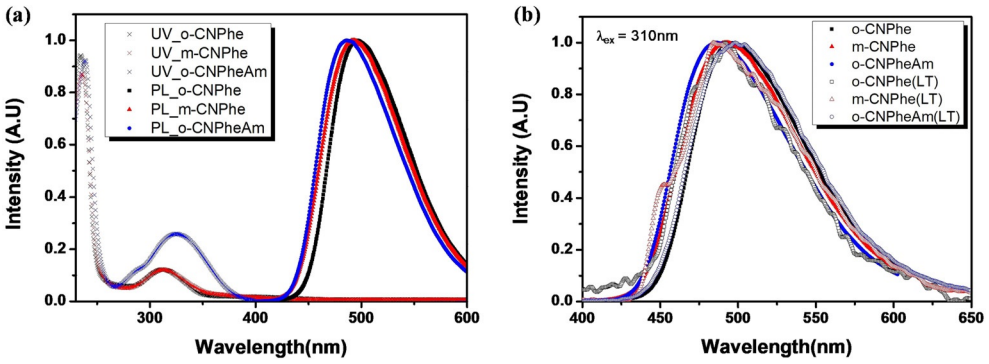

Figure 2. a) Normalized UV/Vis and photoluminescence (PL) characterization of *o*-CNPhe, *m*-CNPhe, and *o*-CNPheAm. b) Normalized PL and low-temperature PL (LTPL) of CNPhe, *m*-CNPhe, and *o*-CNPheAm in toluene.

glet/triplet energy (Figure 2(b)). The singlet energy of *o*-CNPhe, *m*-CNPhe, and *o*-CNPheAm corresponding to the emission from the CT singlet excited state was estimated to be 2.80, 2.82, and 2.82 eV, respectively, from the onset energy of the fluorescence. The singlet energy of *o*-CNPheAm was not decreased, although an additional diphenylamine donor was substituted at the 4-position because the diphenylamine is a relatively weak donor compared with phenoxazine. The donor character is dominated by the phenoxazine donor and the diphenylamine donor has negligible effect on the singlet energy. The singlet energy was slightly increased due to the weakened acceptor character of benzonitrile by diphenylamine. The triplet energy of *o*-CNPhe, *m*-CNPhe, and *o*-CNPheAm was calculated to be 2.80, 2.80, and 2.76 eV, respectively, from the onset energy of phosphorescence. The triplet energy of *o*-CNPheAm was relatively low because of the diphenyl donor at the 4-position. The ΔE_{ST} of *o*-CNPhe, *m*-CNPhe, and *o*-CNPheAm was 0.00, 0.02, and 0.06 eV, respectively.[38,40] The photophysical properties of TADF emitters are summarized in Table 1.

Table 1. Summarization of the photophysical properties of three TADF molecules.

Emitters	HOMO[a] [eV]	LUMO[b] [eV]	B.G.[c]	S_1[d] [eV]	T_1[e] [eV]	ΔE_{ST}[f] [eV]	PLQY[g] [%]	Decay time [μs]
o-CNPhe	−5.72	−2.24	3.48	2.80	2.80	0.00	66.4	2.4
m-CNPhe	−5.78	−2.37	3.41	2.82	2.80	0.02	49.8	4.6
o-CNPheAm	−5.54	−2.30	3.24	2.82	2.76	0.06	81.0	8.9

[a] Onset point of oxidation (IP). [b] HOMO + B.G. [c] Edge of UV. [d] Onset point of 1 wt% of solid film with PS. [e] Onset point at low temperature PL. [f] S_1-T_1. [g] Measured under nitrogen of solid film with PS.

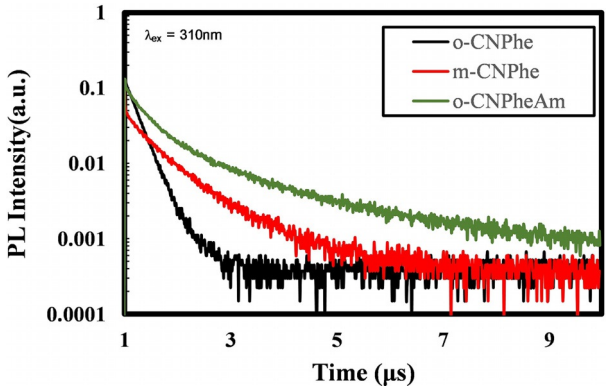

Figure 3. Transient PL decay curves of *o*-CNPhe, *m*-CNPhe, and *o*-CNPheAm at mixed film of mCP:TPBi as host.

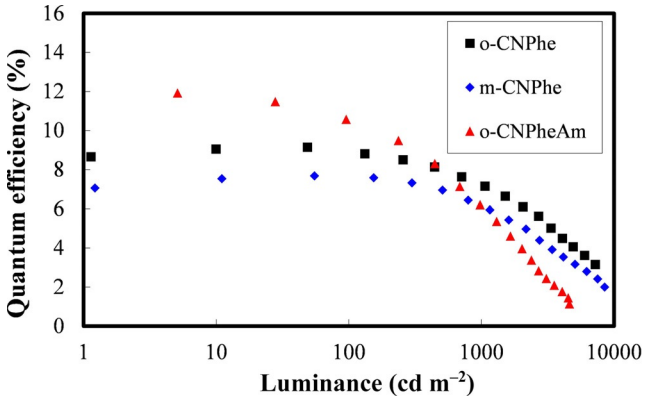

Figure 4. Quantum efficiency-luminance curves of a) *o*-CNPhe, b) *m*-CNPhe, and c) *o*-CNPheAm device.

Transient PL decay curves of TADF emitters are shown in Figure 3. The delayed fluorescence lifetime of *o*-CNPhe, *m*-CNPhe, and *o*-CNPheAm doped films was 2.4, 4.6, and 8.9 μs, respectively, which is correlated very well with their ΔE_{ST} value. PLQY of *o*-CNPhe, *m*-CNPhe, and *o*-CNPheAm doped films was 66.4, 49.8, and 81.0% under nitrogen, respectively. *o*-CNPhe performs better than *m*-CNPhe as anticipated based on their molecular orbital distribution, and *o*-CNPheAm was superior to *o*-CNPhe due to the additional diphenylamine donor and consequentially expanded molecular orbital overlap. A TADF emitter composed of two phenoxazine donors and a phthalonitrile acceptor has been reported that is structurally similar to our TADF molecules.[41] The reported much lower PLQY of 6.4% of that emitter also supports the conclusion that the substitutional position of multiple donors and acceptors is crucial for the TADF properties.

The EQE of the *o*-CNPhe, *m*-CNPhe, and *o*-CNPheAm devices at a doping concentration of 10% are compared in Figure 4. The host material of the devices was a mixed host of 1,3-bis(*N*-carbazolyl)benzene (mCP) and 1,3,5-tris(1-phenyl-1*H*-benzimidazol-2-yl)benzene (TPBi). Current density, luminance, and voltage data are presented in the Supporting Information (Figure S3). The *o*-CNPheAm device showed the highest EQE of 12.0% among the three TADF devices, whereas *o*-CNPhe and *m*-CNPhe devices provided maximum EQE values of 9.0% and 7.7%, respectively. This result agrees with the PLQY of the three TADF emitters, suggesting that the proper substitution point of donor moieties are the LUMO-rich positions of the acceptor for a large HOMO–LUMO overlap favorable for radiative transition process. The efficiency roll-off of *o*-CNPhe and *m*-CNPhe is better than that of *o*-CNPheAm because of relatively short lifetime.

The electroluminescence (EL) spectra of the TADF devices are presented in Figure 5. The λ_{max} of the EL spectra match well with the trend of the relative PL λ_{max}. The EL λ_{max} of *o*-CNPhe, *m*-CNPhe, and *o*-CNPheAm devices were 515, 511, and 509 nm, respectively. Slightly blueshifted emission was observed in the *o*-CNPheAm because of the increased singlet energy, as described in the PL spectra. Therefore, the diphenylamine donor at the 4-position of *o*-CNPheAm increased the EQE of the TADF devices while slightly increasing the emission energy. Device performances are summarized in Table 2.

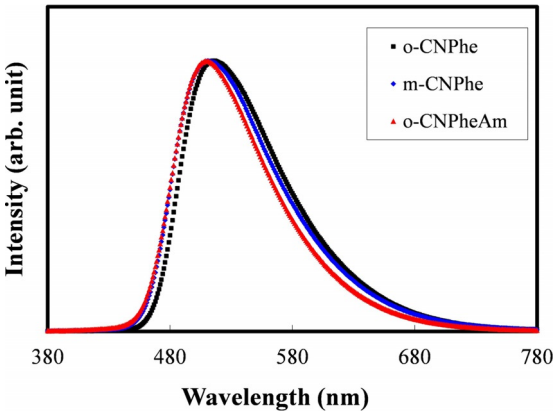

Figure 5. The normalized electroluminescence (EL) spectra of the TADF devices.

Table 2. Summarized device performance of *o*-CNPhe, *m*-CNPhe, and *o*-CNPheAm devices at 10% doping concentration

Host and emitters (doping concentration [%])		Q.E.[a] [%]	C.E.[b] [cd A^{-1}]	P.E.[c] [lm W^{-1}]	Color coordinate (*x*,*y*)
mCP/ TPBi	*o*-CNPhe (10)	9.0	28.3	22.2	(0.33,0.57)
	m-CNPhe (10)	7.7	23.0	18.9	(0.31,0.54)
	o-CNPheAm (10)	12.0	36.1	30.3	(0.30,0.54)

[a] Quantum efficiency. [b] Current efficiency. [c] Power efficiency.

Conclusions

The synthesis and analysis of three TADF emitters with different donor attachment positions, *o*-CNPhe, *m*-CNPhe, and *o*-CNPheAm, revealed that the substitution of strong donors at the positions rendering a large HOMO–LUMO overlap and the addition of a weak donor are an effective design approach to realize TADF emitters having both high efficiency and slightly increased emission energy. The design rule established in this work can be readily applied to the development of high-efficiency TADF emitters with a high emission energy.

Experimental Section

Synthesis

General information: Sodium hydride (60% mineral oil dispersion), dimethyl formamide (DMF), phenoxazine, 1,4-dioxane, tris(dibenzylideneacetone)dipalladium(0), potassium phosphate, and diphenylamine were obtained from Aldrich. Co. 4-Bromo-2,6-difluorobenzonitrile, 2,6-difluorobenzonitrile and 3,5-difluorobenzonitrile were purchased from Alfa Aesar. General analysis of the compounds was carried out according to the reported method.[7]

2,6-Di(10*H*-phenoxazin-10-yl)benzonitrile (*o*-CNPhe)B: Mineral oil dispersion of sodium hydride (60%, 0.23 g) was washed with hexane three times. After vacuum drying for 2 h, it was stirred in DMF (25 mL) under an argon atmosphere. After 10 min, phenoxazine (0.8 g, 4.4 mmol) was added followed by addition of 2,6-difluorobenzonitrile (0.29 g, 2.1 mmol). The mixture was stirred for 10 h and poured into iced water and filtered. After filtration, the greenish product was obtained as a powder (0.80 g, 82% yield). The crude product was further purified by sublimation. ^{1}H NMR (500 MHz, $CDCl_3$): $\delta = 8.08$ (t, $J = 8.0$ Hz, 1H), 7.69 (d, $J = 8.5$ Hz, 2H), 6.78–6.68 (m, 12H), 5.91 ppm (d, $J = 9$ Hz, 4H); ^{13}C NMR (125 MHz, $CDCl_3$): $\delta = 145.3$, 144.2, 137.7, 133.1, 132.8, 123.7, 123.0, 116.5, 113.1, 112.8 ppm; HRMS (FAB): *m/z* calcd for $C_{31}H_{19}N_3O_2$: 465.1477; found: 465.1477.

3,5-Di(10*H*-phenoxazin-10-yl)benzonitrile (*m*-CNPhe): *m*-CNPhe was synthesized according to the synthetic procedure used for *o*-CNPhe (0.70 g, 72% yield). The final product was further purified by sublimation. ^{1}H NMR (500 MHz, $CDCl_3$): $\delta = 7.77$ (m, 2H), 7.70 (m, 1H), 6.75–6.67 (m, 12H), 5.98 ppm (d, $J = 7.5$ Hz, 4H); ^{13}C NMR (125 MHz, $CDCl_3$): $\delta = 144.3$, 143.7, 139.4, 134.6, 133.2, 123.7, 123.0, 118.0, 116.9, 116.4, 113.5 ppm; HRMS (FAB): *m/z* calcd for $C_{31}H_{19}N_3O_2$: 465.1477; found: 465.1477.

4-(Diphenylamino)-2,6-difluorobenzonitrile: Diphenylamine (0.50 g, 3.0 mmol), 4-bromo-2,6-difluorobenzonitrile (0.71 g, 3.3 mmol), $Pd_2(dba)_3$ (0.27 g, 0.3 mmol), tri-*tert*-butylphosphine (0.06 mL, 0.2 mmol), and sodium-*tert*-butoxide (0.85 g, 8.9 mmol) were dissolved in toluene (30 mL), and the mixture was refluxed for 12 h and cooled to RT. The mixture was filtered, extracted with ethyl acetate, and purified by column chromatography using *n*-hexane/ethyl acetate (20:1). The product was obtained as a powder (0.38 g, 42% yield). ^{1}H NMR (500 MHz, DMSO): $\delta = 7.49$ (t, $J = 7.75$ Hz, 2H), 7.36–7.32 (m, 3H), 6.32 ppm (d, $J = 11.0$ Hz, 1H).

4-(Diphenylamino)-2,6-di(10*H*-phenoxazin-10-yl)benzonitrile (*o*-CNPheAm): *o*-CNPheAm was synthesized as described for the synthesis of *o*-CNPhe except that 4-(diphenylamino)-2,6-difluorobenzonitrile (0.25 g, 0.8 mmol) was used instead of 2,6-difluorobenzonitrile. The product was obtained as a powder (0.28 g, 54% yield), which was further purified by sublimation. ^{1}H NMR (500 MHz, $CDCl_3$): $\delta = 7.39$–7.34 (m, 2H), 7.25–7.21 (m, 2H), 6.74–6.62 (m, 8H), 6.10–6.04 ppm (m, 2H); ^{13}C NMR (125 MHz, $CDCl_3$): $\delta = 155.7$, 145.9, 145.5, 145.4, 145.2, 144.8, 144.1, 143.7, 132.0, 130.6, 130.5, 126.7, 125.7, 124.0, 123.4, 123.2, 122.7, 122.6, 121.6, 120.8, 116.4, 116.3, 115.5, 113.6, 112.8 ppm. HRMS (FAB): *m/z* calcd for $C_{43}H_{28}N_4O_2$: 632.2212; found: 632.2216.

Device fabrication and measurements

All devices were fabricated using a thermal evaporator with a vacuum pressure of 1.0×10^{-6} torr. The device structure was indium tin oxide (150 nm) / poly(3,4-ethylenedioxythiophene):poly(styrenesulfonate) (PEDOT:PSS, 60 nm) / 4,4′-cyclohexylidenebis[*N*,*N*-bis(4-methylphenyl)aniline] (TAPC, 20 nm) / (mCP, 10 nm) / mCP:(TPBi):-TADF emitters (45:45:10%, 25 nm) / diphenylphosphine oxide-4-(triphenylsilyl)phenyl (TSPO1, 5 nm) / TPBi (40 nm) / LiF(1.5 nm) / Al (200 nm). Device measurement was performed by sweeping voltage with a Keithley 2400 electrical source and CS2000 spectroradiometer.

Acknowledgements

We acknowledge the financial support from National Science Foundation (DMREF DMR 1435965). The work at SKKU was supported by Basic Science Research Program (Grant No. 2016R1A2B3008845) through the National Research Foundation of Korea funded by the Ministry of Science, ICT, and Future Planning.

Conflict of interest

The authors declare no conflict of interest.

Keywords: electronic structure · energy conversion · fluorescence · OLEDs · TADF

[1] M. A. Baldo, D. F. O'Brien, Y. You, A. Shoustikov, S. Sibley, M. E. Thompson, S. R. Forrest, *Nature* **1998**, *395*, 151.
[2] M. A. Baldo, D. F. O'Brien, M. E. Thompson, S. R. Forrest, *Phys. Rev. B: Condens. Matter Mater. Phys.* **1999**, *60*, 14422.
[3] L. Xiao, S.-J. Su, Y. Agata, H. Lan, J. Kido, *Adv. Mater.* **2009**, *21*, 1271.
[4] S. Su, H. Sasabe, Y. Pu, K. Nakayama, J. Kido, *Adv. Mater.* **2010**, *22*, 3311.
[5] D. H. Kim, N. S. Cho, H.-Y. Oh, J. H. Yang, W. S. Jeon, J. S. Park, M. C. Suh, J. H. Kwon, *Adv. Mater.* **2011**, *23*, 2721.

[6] J. Ye, C.-J. Zheng, X.-M. Ou, X.-H. Zhang, M.-K. Fung, C.-S. Lee, *Adv. Mater.* **2012**, *24*, 3410.
[7] M. Kim, J. Y. Lee, *Adv. Funct. Mater.* **2014**, *24*, 4164.
[8] H. Uoyama, K. Goushi, K. Shizu, H. Nomura, C. Adachi, *Nature* **2012**, *492*, 234.
[9] J. Lee, K. Shizu, H. Tanaka, H. Nomura, T. Yasuda, C. Adachi, *J. Mater. Chem. C.* **2013**, *1*, 4599.
[10] H. Wang, L. Xie, Q. Peng, L. Meng, Y. Wang, Y. Yi, P. Wang, *Adv. Mater.* **2014**, *26*, 5198.
[11] Q. Zhang, D. Tsang, H. Kuwabara, Y. Hatae, B. Li, T. Takahashi, S. Y. Lee, T. Yasuda, C. Adachi, *Adv. Mater.* **2015**, *27*, 2096.
[12] M. Kim, S. K. Jeon, S.-H. Hwang, J. Y. Lee, *Adv. Mater.* **2015**, *27*, 2515.
[13] P. L. dos Santos, J. S. Ward, M. R. Bryce, A. P. Monkman, *J. Phys. Chem. Lett.* **2016**, *7*, 3341.
[14] T. Miwa, S. Kubo, K. Shizu, T. Komino, C. Adachi, H. Kaji, *Sci. Rep.* **2017**, *7*, 284.
[15] Z. Yang, Z. Mao, Z. Xie, Y. Zhang, S. Liu, J. Zhao, J. Xu, Z. Chi, M. P. Aldred, *Chem. Soc. Rev.* **2017**, *46*, 915.
[16] Y. Liu, C. Li, Z. Ren, S. Yan, M. R. Bryce, *Nat. Rev. Mater.* **2018**, *3*, 18020.
[17] O. Bolton, K. Lee, H.-J. Kim, K. Y. Lin, J. Kim, *Nat. Chem.* **2011**, *3*, 205.
[18] D. Lee, O. Bolton, B. C. Kim, J. H. Youk, S. Takayama, J. Kim, *J. Am. Chem. Soc.* **2013**, *135*, 6325.
[19] M. S. Kwon, D. Lee, S. Seo, J. Jung, J. Kim, *Angew. Chem. Int. Ed.* **2014**, *53*, 11177; *Angew. Chem.* **2014**, *126*, 11359.
[20] M. S. Kwon, Y. Yu, C. Coburn, A. W. Phillips, K. Chung, A. Shanker, J. Jung, G. Kim, K. Pipe, S. R. Forrest, J. H. Youk, J. Gierschner, J. Kim, *Nat. Commun.* **2015**, *6*, 8947.
[21] J.-I. Nishide, H. Nakanotani, Y. Hiraga, C. Adachi, *Appl. Phys. Lett.* **2014**, *104*, 233304.
[22] H. Tanaka, K. Shizu, H. Nakanotani, C. Adachi, *Chem. Mater.* **2013**, *25*, 3766.
[23] S. Y. Lee, T. Yasuda, Y. S. Yang, Q. Zhang, C. Adachi, *Angew. Chem. Int. Ed.* **2014**, *53*, 6402; *Angew. Chem.* **2014**, *126*, 6520.
[24] D. Zhang, M. Cai, Y. Zhang, D. Zhang, L. Duan, *Mater. Horiz.* **2016**, *3*, 145.
[25] Y. J. Cho, S. K. Jeon, B. D. Chin, E. Yu, J. Y. Lee, *Angew. Chem. Int. Ed.* **2015**, *54*, 5201; *Angew. Chem.* **2015**, *127*, 5290.
[26] M. Kim, S. K. Jeon, S.-H. Hwang, S.-S. Lee, E. Yu, J. Y. Lee, *Chem. Commun.* **2016**, *52*, 339.
[27] M. Kim, S. K. Jeon, S.-H. Hwang, S.-S. Lee, E. Yu, J. Y. Lee, *J. Phys. Chem. C* **2016**, *120*, 2485.
[28] T. Hatakeyama, K. Shiren, K. Nakajima, S. Nomura, S. Nakatsuka, K. Kinoshita, J. Ni, Y. Ono, T. Ikuta, *Adv. Mater.* **2016**, *28*, 2777.
[29] K. Kawano, K. Nagayoshi, T. Yamaki, C. Adachi, *Org. Electron.* **2014**, *15*, 1695.
[30] L.-S. Cui, Y.-M. Xie, Y.-K. Wang, C. Zhong, Y.-L. Deng, X.-Y. Liu, Z.-Q. Jiang, L.-S. Liao, *Adv. Mater.* **2015**, *27*, 4213.
[31] Y.-H. Kim, C. Wolf, H. Cho, S.-H. Jeong, T.-W. Lee, *Adv. Mater.* **2016**, *28*, 734.
[32] Y. Seino, S. Inomata, H. Sasabe, Y.-J. Pu, J. Kido, *Adv. Mater.* **2016**, *28*, 2638.
[33] D. R. Lee, M. Kim, S. K. Jeon, S.-H. Hwang, C. W. Lee, J. Y. Lee, *Adv. Mater.* **2015**, *27*, 5861.
[34] W. Li, J. Li, D. Liu, F. Wang, S. Zhang, *J. Mater. Chem. C* **2015**, *3*, 12529.
[35] D. Zhang, M. Cai, Z. Bin, Y. Zhang, D. Zhang, L. Duan, *Chem. Sci.* **2016**, *7*, 3355.
[36] D. R. Lee, J. M. Choi, C. W. Lee, J. Y. Lee, *ACS Appl. Mater. Interfaces* **2016**, *8*, 23190.
[37] Y. Geng, L.-S. Cui, J. U. Kim, H. Nakanotani, C. Adachi, *Chem. Lett.* **2017**, *46*, 1490.
[38] C.-Y. Chan, L.-S. Cui, J. U. Kim, H. Nakanotani, C. Adachi, *Adv. Funct. Mater.* **2018**, *28*, 1706023.
[39] To measure the triplet energy, we conducted the gated PL measurement with a 2 μs delay time at low temperature (77 K). Therefore, the low temperature PL spectra represent phosphorescence: L.-S. Cui, H. Nomura, Y. Geng, J. U. Kim, H. Nakanotani, C. Adachi, *Angew. Chem. Int. Ed.* **2017**, *56*, 1571; *Angew. Chem.* **2017**, *129*, 1593.
[40] The ΔE_{ST} values of these three compounds from DFT calculations are very similar to each other (0.02–0.03 eV) because the dihedral angles between the benzonitrile acceptor and the phenoxazine donor in these molecules are identical at 90°. However, the experimentally measured ΔE_{ST} values are more consistent with the delayed fluorescence lifetime.
[41] Y. Zhang, D. Zhang, M. Cai, Y. Li, D. Zhang, Y. Qiu, L. Duan, *Nanotechnology* **2016**, *27*, 094001.

Manuscript received: November 9, 2018
Accepted manuscript online: November 25, 2018
Version of record online: January 7, 2019